Supplemental Text

Cell lines

SKOV3 were cultured in McCoy's 5A medium (Gibco, USA) and other cell lines were cultured in DMEM medium (Gibco, USA). Media were supplemented with 10% fetal bovine serum, 1% penicillin/streptomycin at 37 ℃ in a humidified atmosphere containing 5% CO_2. Cells in the logarithmic growth phase were used in subsequent experiments.

Cell migration

After cells reached 100% confluence, monolayer cells were wounded by scratching the surface straightly as uniformly as possible with a sterilized 200 μl pipette tip. Then the wells were rinsed three times with PBS and replaced with indicated serum-free media. Images were captured by a digital microscopy (Carl Zeiss Jena, Germany) at each indicated time. Experiments were performed in triplicate.

Cell invasion

The cell invasion assay was performed using a 24-well Transwell chamber (Corning, USA). Cells were harvested and suspended in 100 μl serum-free medium were seeded into the upper chamber with an 8-μm pore size insert pre-coated with Matrigel Matrix (BD Biosciences, USA). The lower chamber was filled with 600 μl medium containing 10% FBS. After incubation for 18 hours, cells were stained with a

Computational analyses and bioinformatics

The CASC15 expression data of ovarian cancer patients of GEO (Gene Expression Omnibus) dataset, were downloaded from an international public repository Gene Expression Omnibus [1-8] (GEO, https://www.ncbi.nlm.nih.gov/geo/, last accessed November 15, 2020). And the CASC15, SMAD3 expression data of ovarian cancer specimens of The Cancer Genome Atlas (TCGA) were extracted from exon expression dataset download from UCSC Cancer Browser [9] (http://genome.ucsc.edu/, last accessed November 15, 2020), which was a suite of web-based tools to visualize, integrate and analyze cancer genomics and associated clinical data. The expression quantification was done by averaging the expression of its exons.

Potential miRNA targets on CASC15, SMAD3 and HNF1B mRNAs were predicted by the computer algorithm TargetScanHuman 7.2 [10] (http://www.targetscan.org/vert_72/, last accessed November 15, 2020), DIANA tools [11, 12] (http://carolina.imis.athena-innovation.gr/diana_tools/web/index.php, last accessed November 15, 2020) and starBase v3.0 [13] (http://starbase.sysu.edu.cn/, last accessed November 15, 2020). The mature miRNA sequences used in this study were download from miRBase [14] (http://www.mirbase.org/, last accessed November 15, 2020).

To identify putative transcription factor binding sites in DNA sequences, we analyzed the SMAD3 and CASC15 promoter in PROMO (TRANSFAC v8.3) [15] (http://alggen.lsi.upc.es/cgi-bin/promo_v3/promo/promoinit.cgi?dirDB=TF_8.3, last

Figure S4. CASC15 didn't upregulate SMAD2 expression through miR-23b-3p/miR-24-3p sequestration. (A) The sequence logo of the HNF1B position frequency matrix in the JASPAR database. (B) The sequence logos of the SMAD3 position frequency matrix SMAD2::SMAD3::SMAD4 (left) and SMAD3 (right) in the JASPAR database. (C) Expression of SMAD3 in SKOV3 and ES-2 cells 48 h post SMAD3 siRNA transfection as determined by RT-qPCR and western blots. (D) Expression of SMAD2, SMAD3, and SMAD4 in si-NC or si-C2/si-C5 transfected SKOV3 cells as determined by RT-qPCR. (E) Expression of SMAD2, SMAD3, and SMAD4 in miR-23b-3p or miR-24-3p mimics transfected SKOV3 cells as determined by RT-qPCR and western blots. GAPDH serves as the internal control in RT-qPCR and western blots. ns, no statistical significance, * p <0.05, ** p <0.01, *** p <0.001. Values are mean ± SEM. Data are representative of three independent experiments.

Table S1. List of siRNA sequences.

siRNA	sense (5'→3')	antisense (5'→3')
Negative control	UUCUCCGAACGUGUCACGUTT	ACGUGACACGUUCGGAGAATT
Si-CASC15-1	GACAGUCAGAAUGACUGAUTT	AUCAGUCAUUCUGACUGUCTT
Si-CASC15-2	GAUUUGUCCAGGAGCAGAUTT	AUCUGCUCCUGGACAAAUCTT
Si-CASC15-3	GAAGUACCCUCAGGUGACUTT	AGUCACCUGAGGGUACUUCTT
Si-CASC15-4	GGGAAUUCUCCACCUUAAATT	UUUAAGGUGGAGAAUUCCCTT
Si-CASC15-5	GUGACUACAGAUGUGUUAATT	UUAACACAUCUGUAGUCACTT
Si-HNF1B-1	AUCACUUCCUCCUCAACAAUC	GAUUGUUGAGGAGGAAGUGAU
Si-HNF1B-2	AGUCAGCACCUUGACGAAUAU	AUAUUCGUCAAGGUGCUGACU
Si-HNF1B-3	ACAGCCUCUCCCACCAUAAUC	GAUUAUGGUGGGAGAGGCUGU
Si-HNF1B-4	CCGUACUGUCUAUGUUGUGAU	AUCACAACAUAGACAGUACGG
Si-HNF1B-5	CAGUCCAGAGUUCUGGAAAUA	UAUUUCCAGAACUCUGGACUG
Si-SMAD3-1	CCCAGCACAUAAUAACUUGGA	UCCAAGUUAUUAUGUGCUGGG
Si-SMAD3-2	UCCGCAUGAGCUUCGUCAAAG	CUUUGACGAAGCUCAUGCGGA
Si-SMAD3-3	GAGCCUGGUCAAGAAACUCAA	UUGAGUUUCUUGACCAGGCUC

Table S2. List of shRNA sequences.

shRNA	sense (5'→3')
sh-NC	CCTAAGGTTAAGTCGCCCTCGCTCGAGCGAGGGCGACTTAACCTTAGG
sh-CASC15	AAGATTTGTCCAGGAGCAGATCTCGAGATCTGCTCCTGGACAAATCTT

Table S3. List of mRNA primer sequences.

Target gene	Forward primer (5'→3')	Reverse primer (5'→3')
CASC15	TCCAAGTGTGACTGCCAAGA	CATTTCCTCTGGGTTTTCCA
ZEB1	AAGTGGCGGTAGATGGTAATGT	AAGGAAGACTGATGGCTGAAAT
N-Cadherin	ATGGGAAATGGAAACTTGATGGC	TGGAAAGCTTCTCACGGCAT
Slug	AACAGTATGTGCCTTGGGGG	AAAAGGCACTTGGAAGGGGT
Snail	CTCGGACCTTCTCCCGAATG	AAAGTCCTGTGGGGCTGATG
E-Cadherin	ACAGCACGTACACAGCCCTA	GCAGAAGTGTCCCTGTTCCAG
Claudin-1	TTTACTCCTATGCCGGCGAC	GAGGATGCCAACCACCATCA
SMAD3	AGGGCTTTGAGGCTGTCTACC	GTGCTGGTCACTGTCTGTCTCCT
HNF1B	CCTCCGACAGTTCAGTCAACA	CTTGCTGGGGTTCTTTTGCC
SMAD2	GCCTTTACAGCTTCTCTGAACAA	ATGTGGCAATCCTTTTCGAT
SMAD4	GCTGCAGAGCCCAGTTTAGA	CCCCAAAGCAGAAGCTACGA
GAPDH	CACCCACTCCTCCACCTTTG	CCACCACCCTGTTGCTGTAG

Table S4. List of microRNA primer sequences.

microRNA	3' specific primer (5'→3')
hsa-miR-23b-3p	ATCACATTGCCAGGGATTACCAC
hsa-miR-24-3p	TGGCTCAGTTCAGCAGGAACAG
hsa-miR-27b-3p	TTCACAGTGGCTAAGTTCTGC

MicroRNA specific 5' primer, U6-Forward and U6-Reverse were provided by the Mir-X™ miRNA First Strand Synthesis Kit (Takara, Japan).

Table S5. Schema of miR-23b-3p, miR-24-3p and miR-27b-3p binding sites in predicted target 3' UTR sequences of human genes.

Gene	microRNA	Target Site	3' UTR Position
CASC15	miR-23b-3p		chr6:22147894-22147916
CASC15	miR-24-3p	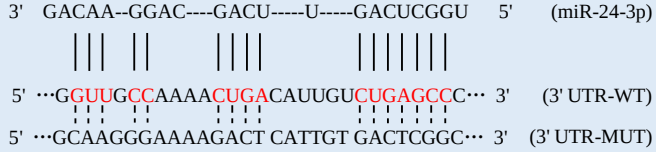	chr6:22149601-22149627
CASC15	miR-27b-3p		chr6:22147507-22147530
SMAD3	miR-23b-3p	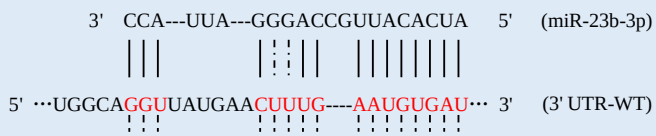	chr15:67485127-67485148
HNF1B	miR-23b-3p	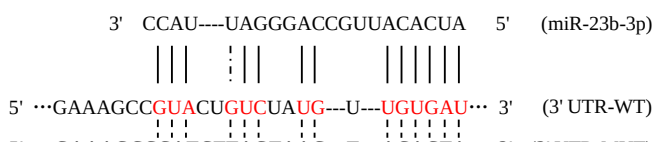	chr17:36047060-36047078
HNF1B	miR-24-3p	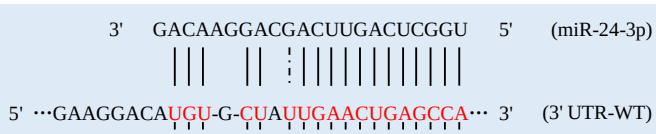	chr17:36046978-36046997

Putative binding sites were mutated and highlighted in red.

Table S6. The predicted HNF1B-binding sites on the SMAD3 promoter.

	Matrix Name	Predicted sequence	Start	End
HNF1B-binding site 1	HNF1B	TTTTTTTTTAAC	-1430	-1419
HNF1B-binding site 2	HNF1B	GTTAAAAACAAAC	-1387	-1375
HNF1B-binding site 3	HNF1B	TTCAAAGATAAAT	-1033	-1021

Table S7. The predicted SMAD3-binding sites on the CASC15 promoter.

	Matrix Name	Predicted sequence	Start	End
SMAD3-binding site 1	SMAD2::SMAD3::SMAD4	GCGGCTCACACCC	-1985	-1973
SMAD3-binding site 2	SMAD3	CGTCCAGACT	-1867	-1858
SMAD3-binding site 3	SMAD2::SMAD3::SMAD4	CCGTCTACCTCAT	-1397	-1385

References

1. Barrett T, Wilhite SE, Ledoux P, Evangelista C, Kim IF, Tomashevsky M, et al. NCBI GEO: archive for functional genomics data sets-update. Nucleic Acids Research. 2013; 41: D991-D5.
2. Tothill RW, Tinker AV, George J, Brown R, Fox SB, Lade S, et al. Novel molecular subtypes of serous and endometrioid ovarian cancer linked to clinical outcome. Clin Cancer Res. 2008; 14: 5198-208.
3. Mateescu B, Batista L, Cardon M, Gruosso T, de Feraudy Y, Mariani O, et al. miR-141 and miR-200a act on ovarian tumorigenesis by controlling oxidative stress response. Nat Med. 2011; 17: 1627-35.
4. King ER, Tung CS, Tsang YT, Zu Z, Lok GT, Deavers MT, et al. The anterior gradient homolog 3 (AGR3) gene is associated with differentiation and survival in ovarian cancer. Am J Surg Pathol. 2011; 35: 904-12.
5. Ferriss JS, Kim Y, Duska L, Birrer M, Levine DA, Moskaluk C, et al. Multi-gene expression predictors of single drug responses to adjuvant chemotherapy in ovarian carcinoma: predicting platinum resistance. PLoS One. 2012; 7: e30550.
6. Konstantinopoulos PA, Spentzos D, Karlan BY, Taniguchi T, Fountzilas E, Francoeur N, et al. Gene expression profile of BRCAness that correlates with responsiveness to chemotherapy and with outcome in patients with epithelial ovarian cancer. J Clin Oncol. 2010; 28: 3555-61.
7. Lisowska KM, Olbryt M, Dudaladava V, Pamula-Pilat J, Kujawa K, Grzybowska E, et al. Gene expression analysis in ovarian cancer - faults and hints from DNA microarray study. Front Oncol. 2014; 4: 6.
8. Mok SC, Bonome T, Vathipadiekal V, Bell A, Johnson ME, Wong KK, et al. A gene signature predictive for outcome in advanced ovarian cancer identifies a survival factor: microfibril-associated glycoprotein 2. Cancer Cell. 2009; 16: 521-32.
9. Kent WJ, Sugnet CW, Furey TS, Roskin KM, Pringle TH, Zahler AM, et al. The human genome browser at UCSC. Genome Research. 2002; 12: 996-1006.
10. Agarwal V, Bell GW, Nam JW, Bartel DP. Predicting effective microRNA target sites in mammalian mRNAs. Elife. 2015; 4.
11. Paraskevopoulou MD, Georgakilas G, Kostoulas N, Vlachos IS, Vergoulis T, Reczko M, et al. DIANA-microT web server v5.0: service integration into miRNA functional analysis workflows. Nucleic Acids Research. 2013; 41: W169-W73.
12. Paraskevopoulou MD, Georgakilas G, Kostoulas N, Reczko M, Maragkakis M, Dalamagas TM, et al. DIANA-LncBase: experimentally verified and computationally predicted microRNA targets on long non-coding RNAs. Nucleic Acids Research. 2013; 41: D239-D45.
13. Li JH, Liu S, Zhou H, Qu LH, Yang JH. starBase v2.0: decoding miRNA-ceRNA, miRNA-ncRNA and protein-RNA interaction networks from large-scale CLIP-Seq data. Nucleic Acids Research. 2014; 42: D92-D7.
14. Kozomara A, Griffiths-Jones S. miRBase: annotating high confidence microRNAs using deep sequencing data. Nucleic Acids Research. 2014; 42: D68-D73.
15. Messeguer X, Escudero R, Farre D, Nunez O, Martinez J, Alba M. PROMO: detection of known transcription regulatory elements using species-tailored searches. Bioinformatics. 2002; 18: 333-4.
16. Khan A, Fornes O, Stigliani A, Gheorghe M, Castro-Mondragon JA, van der Lee R, et al. JASPAR 2018: update of the open-access database of transcription factor binding profiles and its web framework. Nucleic Acids Research. 2018; 46: D260-D6.